JACS
JOURNAL OF THE AMERICAN CHEMICAL SOCIETY

Article

pubs.acs.org/JACS

Effects of Pendant Ligand Binding Affinity on Chain Transfer for 1-Hexene Polymerization Catalyzed by Single-Site Zirconium Amine Bis-Phenolate Complexes

D. Keith Steelman,[†] Silei Xiong,[‡] Paul D. Pletcher,[†] Erin Smith,[†] Jeffrey M. Switzer,[‡] Grigori A. Medvedev,[‡] W. Nicholas Delgass,[‡] James M. Caruthers,*[,‡] and Mahdi M. Abu-Omar*[,†,‡]

[†]Brown Laboratory, Department of Chemistry, Purdue University, 560 Oval Drive, West Lafayette, Indiana 47907, United States

[‡]School of Chemical Engineering, Purdue University, Forney Hall of Chemical Engineering, 480 Stadium Mall Drive, West Lafayette, Indiana 47907, United States

Supporting Information

ABSTRACT: The kinetics of 1-hexene polymerization using a family of five zirconium amine bis-phenolate catalysts, Zr[tBu-ON^{X}O]Bn$_2$ (where X = THF (**1**), pyridine (**2**), NMe$_2$ (**3**), furan (**4**), and SMe (**5**)), has been investigated to uncover the mechanistic effect of varying the pendant ligand X. A model-based approach using a diverse set of data including monomer consumption, evolution of molecular weight, and end-group analysis was employed to determine each of the reaction specific rate constants involved in a given polymerization process. The mechanism of polymerization for **1**−**5** was similar and the necessary elementary reaction steps included initiation, normal propagation, misinsertion, recovery from misinsertion, and chain transfer. The latter reaction, chain transfer, featured monomer independent β-H elimination in **1**−**3** and monomer dependent β-H transfer in **4** and **5**. Of all the rate constants, those for chain transfer showed the most variation, spanning 2 orders of magnitude (ca. (0.1−10) × 10^{-3} s^{-1} for vinylidene and (0.5−87) × 10^{-4} s^{-1} for vinylene). A quantitative structure−activity relationship was uncovered between the logarithm of the chain transfer rate constants and the Zr−X bond distance for catalysts **1**−**3**. However, this trend is broken once the Zr−X bond distance elongates further, as is the case for catalysts **4** and **5**, which operate primarily through a different mechanistic pathway. These findings underscore the importance of comprehensive kinetic modeling using a diverse set of multiresponse data, enabling the determination of robust kinetic constants and reaction mechanisms of catalytic olefin polymerization as part of the development of structure−activity relationships.

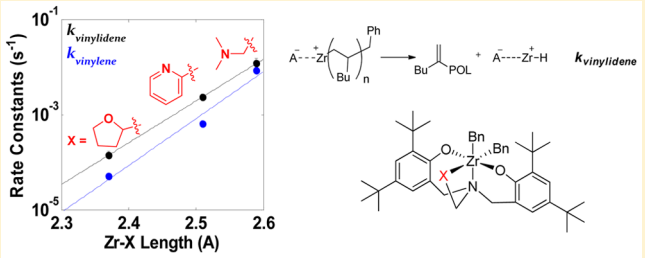

INTRODUCTION

Production of polyolefins is a major industrial process with a current capacity of ca. 110 billion kg per year globally.[1] While polyolefins are primarily produced using heterogeneous Ziegler catalysts, homogeneous single-site catalysts, the so-called metallocenes, have attracted attention because they offer potential control of the various kinetic steps, which in turn can be manipulated by "catalyst design".[2−4] One of the drawbacks of metallocenes, beside sensitivity to polar functional groups, is their thermal sensitivity. Beyond metallocenes, the next generation of thermally stable catalysts includes group 4 coordination complexes featuring phenolate amine ligands.[5] While high-throughput screening has accelerated the discovery process with group 4 coordination complexes leading to Dow's catalysts for olefin block copolymer synthesis,[6] the promise of directly correlating kinetic constants to descriptors of the catalyst has not yet been realized. A major obstacle in the way of rational catalyst design is the lack of proper quantitative kinetic analysis of all the relevant processes (i.e., kinetic steps) that are involved in catalytic olefin polymerization.[7,8] Nevertheless, the study of single-site catalysts for olefin polymerization is particularly attractive because of the potential of correlating directly the physical properties of the resulting polymer to structural features of the catalyst based on first principles.[9] This correlation allows one to draw conclusions on how a catalyst structure may be manipulated to yield specific polymeric architectures.

One specific family of nonmetallocene catalysts, first pioneered by Kol and co-workers, that has sparked interest utilizes an amine bis-phenolate (Salan) ligand system (see Figure 1).[10,11] The reason for choosing this particular family of ligands as part of our detailed kinetic studies is the relative ease of synthesis and the ability to tune the catalyst's coordination environment.[12] Furthermore, these catalysts exhibit high activity, comparable to metallocene catalysts, with 1-hexene in conventional organic solvents such as toluene. This feature enables the collection of kinetic data in the condensed phase and eliminates mass transfer limitations that are inherent with gaseous substrates. Following up on Kol's earlier qualitative

Received: February 8, 2013

   dx.doi.org/10.1021/ja401474v | J. Am. Chem. Soc. XXXX, XXX, XXX−XXX

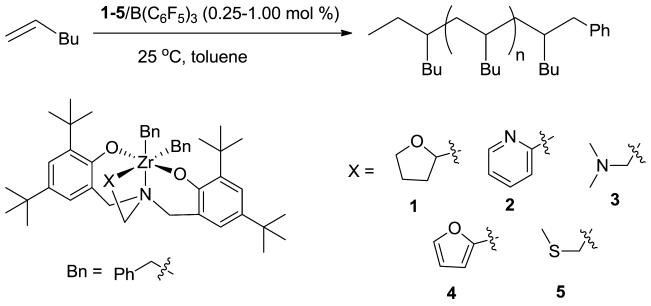

Figure 1. 1-Hexene polymerization catalyzed by zirconium salan-type catalysts **1**−**5** when combined with the activator $B(C_6F_5)_3$.

observations that the nature of the pendant ligand (X) and its distance from the metal center (Zr−X) influence chain transfer,[13] we have undertaken a comprehensive kinetic study of the five catalysts shown in Figure 1. We will show in the following sections the minimally required set of rate constants needed to describe completely the rich data set for each catalyst including the molecular weight evolution. The rate constant affected the most by changing the pendant ligand (X) is that for chain transfer that results in vinyl terminated polymer.

Four chemical mechanisms have been noted for chain transfer in single-site homogeneous olefin polymerization catalysts. Normally chain transfer occurs via β-H elimination to give vinylidene terminated polymer chains. This process is independent of monomer concentration and the resulting metal hydride undergoes reinitiation. If the catalyst is susceptible to 2,1-misinsertion (which results in regio-errors), the resulting polymeryl chain can undergo unimolecular β-H elimination to give vinylene terminated polymer chains.[14] In some cases for propylene, a second mechanism has been recognized in which β-methyl instead of β-H elimination occurs to give M-CH_3, which can reinitiate by inserting a monomer.[15] It should be noted that ethyl or higher alkane elimination has not been observed. A third mechanism is second-order chain transfer in which vinylidene and vinylene end groups result from H-transfer to a monomer.[7,8] In this mechanism the chain transfer rate constant is second-order and the rate is dependent on the monomer concentration. The last recognized chemical mechanism for chain transfer is that to the activator. This is usually a minor pathway observed with aluminum alkyl activators, although exceptions where it is dominant have been noted in the literature.[16]

Suppression of chain transfer while maintaining a high propagation rate can provide easy access to new block copolymers via controlled sequential addition of monomer.[17] Therefore, quantitative understanding of factors that control the rate of chain transfer exclusively is valuable from a fundamental standpoint as well as for practical applications. In semiquantitative studies, two parameters, catalyst activity (TOF or g polymer mol^{-1} catalyst h^{-1}) that is taken as indicative of the propagation rate constant and the molecular weight average of the resulting polymer (M_w), have been used to infer how catalyst structure influences the chain transfer rate. The consensus from these studies pointed to steric bulk as the major contributor to retardation of chain transfer as long as there is a weakly coordinating ligand or an available coordination site for monomer docking.[18] Bercaw and co-workers observed that the use of a more open metal center leads to faster propagation by allowing more space for a more facile monomer insertion and an increase in the propensity for β-H elimination due to more available space to accommodate the β-H agostic bonding interactions necessary for β-H elimination.[19] This empirical insight has been responsible for the development of late transition metal catalysts based on Fe, Co, and Ni that can effect ethylene polymerization rather than producing oligomers.[18]

Ziegler and co-workers performed a detailed computational study of ethylene polymerization using a wide range of d^0 metal catalysts,[20] finding that the energy barrier for chain transfer is strongly influenced by sterically bulky ligands and, to some degree, the identity of the metal. They also observed that, for the systems studied, β-H transfer to monomer, a second-order chain transfer process, is preferred over β-H elimination, except when monomer concentration is small or when monomer coordination to the metal is severely hindered. This observation was used successfully by Busico and co-workers to design catalysts that were shown experimentally to have hindered chain transfer reactions.[21] In addition, Camacho and Guan have attributed the steric blocks present in their cyclophane-based nickel catalyst to its ability to polymerize olefins even at high temperatures where chain transfer typically dominates,[22] and Rieger and co-workers have used sterically hindered nickel and palladium catalysts to produce high molecular weight polyethylene rather than α-olefin oligomers.[23]

Earlier work by Doi and co-workers showed that for $V(acac)_3$−$Al(C_2H_5)_2Cl$ the identity of the alkylaluminum cocatalyst influences the amount of chain transfer.[24] Later work by Naga and Mizunuma showed similar activator effects on the amount of chain transfer using zirconium metallocenes, with an additional observation that the β-H chain transfer pathway was preferred with one alkylaluminum activator while chain transfer to activator was dominant with another.[25] More

Table 1. Rate Constants for 1-Hexene Polymerization with the Zr[tBu-ON^{X}O]Bn_2/$B(C_6F_5)_3$ Catalysts 1−5[a]

X	THF (1)	Pyridine (2)	NMe2 (3)	Furan (4)	SMe[b] (5)
Zr−X/ Å	2.37	2.51	2.59	2.69	2.89
k_i/ M^{-1} s^{-1}	0.08 (+0.02/ −0.01)	>0.05	0.16 (+0.04/-0.02)	0.0031 (+0.0003/-0.0004)	0.017 (+0.002/-0.001)
k_p/ M^{-1} s^{-1}	8.0 (+0.8/ −0.2)	1.8 (+0.2/-0.1)	11 (+1/-1)	3.52 (+0.03/-0.04)	12 (+5/-4)
k_{mis}/ M^{-1} s^{-1}	0.054 (+0.026/-0.003)	0.031 (+0.004/-0.005)	0.055 (+0.007/-0.004)	0.0064 (+0.0002/-0.0004)	0.20 (+0.08/-0.06)
k_{rec}/ M^{-1} s^{-1}	0.047 (+0.021/-0.002)	0.028 (+0.004/-0.005)	0.04 (+0.03/-0.02)	0[c]	0.036 (+0.001/-0.001)
$k_{vinylidene}$ (10^{-3})/ s^{-1}	0.14 (+0.014/ −0.02)	2.4 (+0.1/-0.1)	12.2 (+0.8/-0.6)	1.00 (+0.07/-0.08)	0
$k_{vinylene}$ (10^{-3})/ s^{-1}	0.051 (+0.002/ −0.003)	0.65 (+0.06/ −0.05)	8.72 (+0.07/ −0.04)	0	0
$k_{vinylidene}$ (10^{-3})/ M^{-1} s^{-1}	0	0	0	12.1 (+0.7/-0.6)	2.2 (+0.6/-0.4)
$k_{vinylene}$ (10^{-3})/ M^{-1} s^{-1}	0	0	0	6.9 (+0.07/-0.06)	0.95 (+0.06/-0.04)

[a]In toluene at 25 °C. See Figure 1 for precatalyst structures and Scheme 1 for reactions steps. Errors are in parentheses. [b]In toluene at 22 °C. [c]A value of zero means the fit did not require the inclusion of this reaction step.

dx.doi.org/10.1021/ja401474v | J. Am. Chem. Soc. XXXX, XXX, XXX−XXX

recently, Marks and co-workers have studied the effects of ion pair structure and dynamics on polymerization activity, stereoselectivity, and chain transfer in C_s-symmetric zirconium metallocene precatalysts using various fluorinated aryl borane and aluminum activators.[26] They found that ion pairing dictates the relative rate of termination to propagation as well as the preferred termination pathway.

In this study, we describe a detailed kinetic analysis for catalysts **1**−**5**, culminating in Table 1, which contains all of the rate constants for each system. The following sections will discuss observations and trends that only become apparent through the generation and examination of the full kinetic constants presented in Table 1. These kinetic constants represent the minimal number of necessary reaction steps needed to describe the entire data set for each of the catalysts, which includes monomer consumption kinetics, molecular weight evolution as determined by GPC (gel permeation chromatography), active-site count, and analysis of terminated end groups in the resulting polymer. The mechanism of chain transfer and its corresponding rate constants as the pendant ligand (X) changes have been pinpointed. A linear quantitative structure−activity relationship (QSAR) between the logarithm of the chain transfer rate constant and the Zr−X bond length will be shown and discussed.

EXPERIMENTAL PROCEDURES

General Procedure. All manipulations were performed under dry inert atmosphere in a glovebox or at a vacuum manifold using air sensitive techniques under N_2 or Ar atmosphere. Toluene and pentane were distilled over activated alumina and a copper catalyst using a solvent purification system (Anhydrous Technologies) and degassed through freeze−pump−thaw cycles. Both solvents were stored over activated molecular sieves. Tetrabenzylzirconium was purchased from STREM and used as received. The monomer 1-hexene was purchased from Aldrich and purified by distillation over a small amount of dimethyl bis(cyclopentadienyl)zirconium and stored over molecular sieves. Tris(pentafluorophenyl)boron was purchased from STREM and purified by sublimation. Diphenylmethane was purchased from Aldrich and stored over molecular sieves. CH_3OD was purchased from Cambridge Isotopes and used as received. d_8-Toluene was used as received and stored over molecular sieves. ^1H and ^2H NMR experiments were performed on a Varian INOVA600 MHz or Bruker DRX500 MHz spectrometer.

The ligands and precatalysts (**1**−**5**) were prepared following modified literature procedures.[12,27,28] We describe herein the details for one representative procedure and provide the others in the Supporting Information.

Synthesis of 6,6′-((((Tetrahydrofuran-2-yl)methyl)-azanediyl)bis(methylene))bis(2,4-di-*tert*-butylphenol), tBu-ON^{THF}O ligand. In a typical synthesis, an 80 mL reaction vessel was charged with 2,4-di-*tert*-butylphenol (6.19 g, 30.0 mmol), 2-(aminomethyl)tetrahydrofuran (1.55 mL, 15 mmol), and 37% histological grade formaldehyde (6.00 mL, 80 mmol), distilled water, and a stir bar while maintaining a maximum volume of 80 mL. The biphasic reaction mixture was placed in a CEM microwave reactor and allowed to warm to 100 °C over 5 min while stirring. The reaction was allowed to stand at 100 °C for 30 min, and then cooled to room temperature. The aqueous layer was removed, and cold, dry methanol was added to the organic phase. This mixture was shaken for 30 min, and the resulting solid isolated by vacuum filtration. The crude ligand product was purified by crystallization from ethanol (28% yield).

Synthesis of Zr[tBu-ON^{THF}O]Bn$_2$ (1). In a typical synthesis, a 100 mL flask was charged with tetrabenzylzirconium (0.557 g, 1.22 mmol), 20 mL toluene, and a stir bar and fitted with a rubber septum. A second 100 mL flask was charged with the ^{t}Bu-ON^{THF}O ligand (0.609 g, 1.13 mmol) and 20 mL of toluene. The two flasks were placed under an inert atmosphere, and the ligand solution was added to the tetrabenzylzirconium solution via a cannula. The reaction was allowed to warm to 60 °C and stir for 2 h resulting in a bright yellow solution. The solution was concentrated to about 10 mL and placed into a −10 °C freezer. Yellow crystals formed within 2 days and the mother liquor was removed via a cannula. The crystals were dried under vacuum (84% yield). The precatalyst was recrystallized by vapor diffusion of pentane into a precatalyst/toluene solution to afford an analytically pure complex.

NMR Scale Polymerization of 1-Hexene. The procedure for NMR scale polymerization is based on the literature.[29] For a typical polymerization, Zr[tBu-ON^{THF}O]Bn$_2$ (**1**) (6.1 mg, 0.0075 mmol) was dissolved in 0.5 mL toluene in a small vial and sealed with a screw-cap septum. The vial containing the precatalyst solution was pierced with a 1 mL syringe. The vial and syringe were placed in an N_2 bag and allowed to equilibrate to 25 °C. Tris(pentafluorophenyl)boron (4.3 mg, 0.0084 mmol), 1-hexene (0.1265 g, 1.50 mmol), and diphenylmethane (9.5 mg 0.056 mmol) were added to a 2 mL volumetric flask and diluted to the mark with d_8-toluene. This solution was placed in an NMR tube and sealed with a septum. The monomer/activator solution was placed in the spectrometer and allowed to equilibrate to 25 °C using a VT controller. A measurement was taken to determine the initial concentration of monomer relative to the internal standard. The NMR tube was removed from the spectrometer, and the catalyst precursor solution was added to the activator/monomer solution by piercing the septum while the syringe remained in the N_2 bag. The reaction mixture was shaken for ca. 30 s and placed back into the spectrometer. Spectra were acquired at predetermined time intervals until the reaction reached completion. Each sample was prepared for GPC analysis by evaporation over mild heat before dissolution in hexanes and filtration through an alumina plug to remove the quenched catalyst. Evaporation of solvent yielded clear, colorless poly(1-hexene). The array of ^1H spectra was collected on an INOVA 600 MHz spectrometer and analyzed using MestReNova.

Batch Polymerization of 1-Hexene. The procedure for Manual Quench is based on literature.[30] For a typical polymerization, Zr[tBu-ON^{THF}O]Bn$_2$ (0.073 g, 0.090 mmol) was dissolved in 5.0 mL toluene in a small vial that was sealed with a screw-cap septum. The vial containing the precatalyst solution was pierced with a 10 mL syringe. The vial and syringe were placed in an N_2 bag and allowed to equilibrate to 25 °C. Tris(pentafluorophenyl)boron (0.053 g, 0.099 mmol), and 1-hexene (1.575 g, 18.71 mmol) were added to a 25 mL flask and diluted to the mark with toluene. This solution was diluted to 26 mL with 1 mL of toluene, and 1 mL of the resulting solution was removed for quantification of the initial monomer concentration through NMR analysis. The flask was sealed with a septum and moved from an N_2 filled glovebox to a vacuum manifold and placed under argon. The monomer/activator solution was allowed to equilibrate to 25 °C using a temperature-controlled silicone oil bath. The catalyst precursor solution was added to the activator/monomer solution by piercing the septum while the syringe remained in the N_2 bag. The resulting yellow solution was allowed to stir while aliquots were removed at selected times and each was injected into a 10 mL volumetric flask containing 1 mL of deutero-methanol. A 1 mL aliquot from the quenched solutions was removed and a 0.5 mL solution of *d*-toluene spiked with diphenylmethane as an internal standard for quantification of 1-hexene consumption (via ^1H NMR on Varian Inova 600). Each sample was prepared for GPC analysis by evaporation over mild heat before dissolution in hexanes and filtration through an alumina plug to remove the quenched catalyst. Evaporation of solvent yielded clear, colorless poly(1-hexene).

In the case of vinyl end group analysis, a 1 mL aliquot was worked up as described above. The resulting polymer was dissolved in $CDCl_3$, and diluted to the mark in a 2 mL volumetric flask. Diphenylmethane was used as an internal standard and the method of standard additions was used in quantification of the end groups by ^1H NMR. All end-group analysis measurements were taken on a Bruker DRX500 spectrometer at 25 °C.

In the case of ^2H analysis for active-site counting, the remaining quenched reaction solution (8 mL) was worked up as described above. The resulting polymer was dissolved in CH_2Cl_2, and diluted to the

dx.doi.org/10.1021/ja401474v | J. Am. Chem. Soc. XXXX, XXX, XXX−XXX

mark in a 2 mL volumetric flask. d_6-Benzene was used as an internal standard and the method of standard additions was used in quantification of active sites by ^{2}H NMR. All active site measurements were taken on a Bruker DRX500 spectrometer at 25 °C.

Gel Permeation Chromatography (GPC) Analysis. The procedure used to analyze polymer samples using GPC methods was taken from Novstrup et al.,[7] and it is summarized below. Poly(1-hexene) samples were added to THF at room temperature and allowed to dissolve for 4 h. Solutions were then passed through a 0.2 μm filter to remove any particulate matter. The GPC analysis was performed on a Waters GPCV 2000 for system **1** and **3**, and on a Viscotek GPCmax VE 2001 for system **2**, **4**, and **5**. On the Waters GPCV 2000, samples were injected through a 101.3 μL injection loop and passed through two Polymer Laboratories PLGel 5 μm Mixed-C columns in series in a 45 °C oven at a flow rate of 1.0 mL min^{-1}. On Viscotek GPCmax VE 2001, samples were injected through a 200 μL injection loop and passed through three Viscotek T6000 M 10 μm General Mixed Org columns in series in a 35 °C oven at a flow rate of 1.0 mL min^{-1}. The analysis made use of the differential RI detector and a capillary viscometer. Molecular weights were assigned by way of a universal calibration curve created with polystyrene standards ranging from 580 g mol^{-1} to 3 114 000 g mol^{-1}. The calibration was verified through the analysis of a broad standard, SRM 706a, provided by the National Institute of Standards and Technology.

RESULTS

Here we present a complete kinetic analysis for 1-hexene polymerization by catalysts **1**−**5**. In approaching each system, we followed our previously developed kinetic modeling method[7,29] based on the analysis of multiresponse data that includes GPC traces where we did not make any a priori assumptions about the elementary reaction steps taking place. However, when this independent analysis was completed for each catalyst system, it emerged that all five systems described herein follow a similar kinetic mechanism including initiation, propagation via normal insertion, 2,1-misinsertion, recovery from misinsertion, and two types of chain transfer resulting in the formation of vinylidene and vinylene species. The kinetic steps are illustrated in Scheme 1. The activation step is fast on the time scale of polymerization and as a result was not used in the kinetic modeling. Chain transfer resulting in vinylidene and vinylene follows either unimolecular (monomer independent) β-H elimination or bimolecular β-H transfer to monomer.

Examining the available data, the reasons for the mechanism above (Scheme 1) are as follows:

I. Misinsertion (k_{mis}) and recovery (k_{rec}) are necessary because of the following:

1. We observe two types of chains attached to the active sites (primary and secondary) in active-site counting experiments with MeOD quenches (^{2}H NMR of isolated polymer gives δ 0.83 (DH_2C−Polymer) and 1.22 (DH(Bu)C−Polymer).
2. When analyzing the produced polymer, there are two types of vinyl end groups observed: one with a terminal double bond at the end of the chain (vinylidene), and another with an internal double bond inside the chain (vinylene). We believe, in agreement with the literature,[30] that the latter arises from chain transfer of misinserted chains.
3. The secondary sites (Zr-CH(Bu)−Polymer) do not accumulate over time. We assume this is the case because they are able to recover via normal 1-hexene insertion.
4. Although there is an alternative explanation for points 1 through 3, namely, that there are two different sites growing separately, it is expected that such a mechanism would at least under some experimental conditions produce bimodal MWD. The fact that none of the five systems exhibit a bimodal MWD and all yield narrow PDI values strongly suggest that these systems are single-site catalysts.

Scheme 1. Elementary Kinetic Steps Used in Fitting the Data for Catalysts 1−5[a]

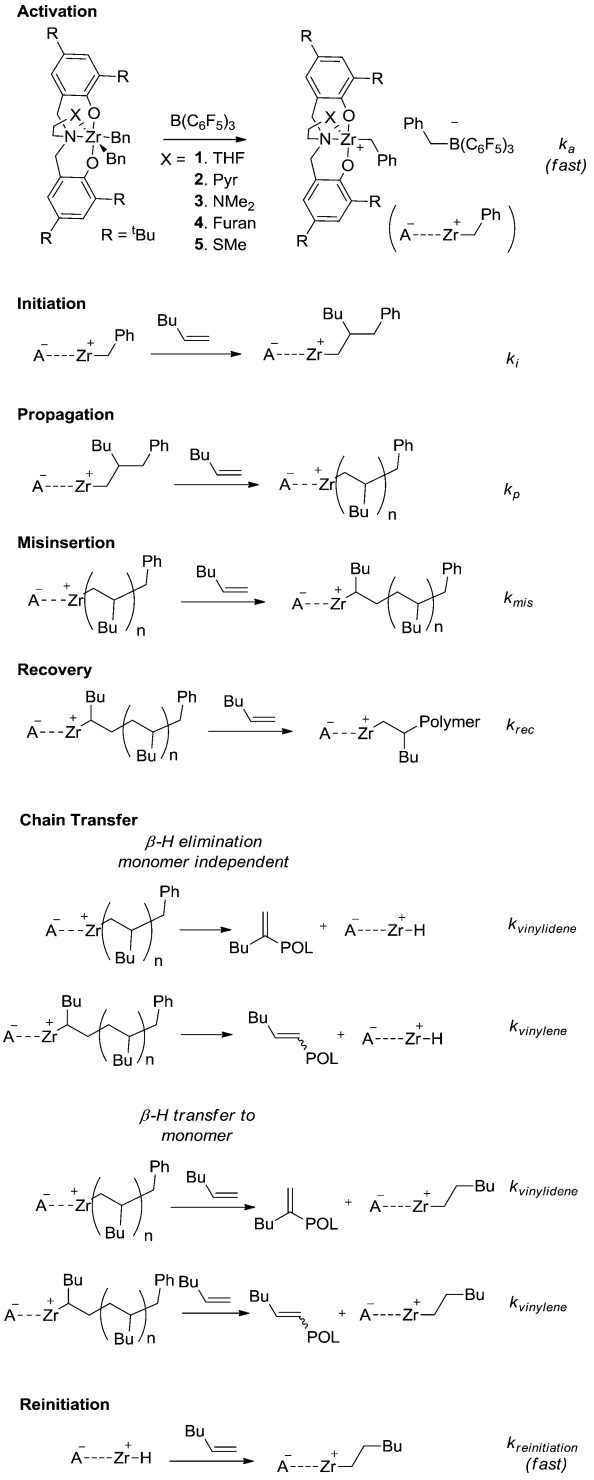

[a]The ordinary differential equations (ODEs) that describe the mass-action kinetics associated with this mechanism are provided in the Supporting Information.

dx.doi.org/10.1021/ja401474v | J. Am. Chem. Soc. XXXX, XXX, XXX−XXX

II. Chain transfer reactions are necessary because we observe polymer chains with vinyl end groups. It should be noted that there are two possible mechanisms through monomer dependent and monomer independent pathways. The monomer dependent pathway (β-H transfer to monomer) results in an active site with one repeat unit, while the monomer independent pathway (β-H elimination) results in the formation of a zirconium hydride. There is an ongoing discussion in the literature whether the insertion of a monomer in the zirconium hydride, i.e., reinitiation ($k_{reinitiation}$) is facile or hindered as compared to the normal initiation (k_i) for a given catalyst system.[31] If the rate constant of reinitiation ($k_{reinitiation}$) of the zirconium hydride is slow, it effectively renders affected catalyst sites inactive, which in turn has an effect on the monomer consumption curve, active sites count, and the MWDs. As a result the value of the reinitiation rate constant ($k_{reinitiation}$) can be determined. On the other hand, when the rate constant of the reinitiation of zirconium hydride is fast, the data are usually not sensitive enough to determine its value precisely, similarly to how the data are not sensitive enough to determine the normal initiation rate when it is not significantly slower than the propagation rate. In practice we have set the reinitiation rate to be equal to the propagation rate in cases when the reinitiation rate is determined to be fast.

An important caveat is that the catalyst participation for each system may vary and not be 100%. The catalyst participation can be estimated from the active site counting experiments (quench with MeOD followed by ^{2}H NMR analysis of polymer chains). Also, for the systems where the chain transfer is low (catalysts **1** and **5**) the catalyst participation is readily estimated from the slope of M_w vs conversion plot, which is linear in these cases. When applicable, these two methods give consistent results. The catalyst participation information for **1**−**5** is provided in the Supporting Information.

For each system we simultaneously fit the following: (1) monomer consumption, (2) MWD, (3) active site counts, and (4) end group counts. The data set usually includes several initial conditions of different $[C]_0$ (C = precatalyst/$B(C_6F_5)_3$) and $[M]_0$ (M = 1-hexene). For some conditions, multiple repeats were carried out, and the results were consistent when small variation in active-site catalyst participation was accounted for; however, only one repeat is shown in the figures below.

In determining error margins of the estimates for the six rate constants for each catalyst system (see Scheme 1), the following considerations apply: (1) the experimental data has an inherent error resulting from the measurement procedure. Specifically, the NMR spectrum is characterized by the uncertainty of roughly 5% for the peak integration; the GPC trace is characterized by the uncertainty of the weight average, M_w, of approximately 3%, where the uncertainty in the shape of the distribution is more difficult to ascertain (see discussion in reference 29). However, these estimates are based on the best experimental conditions, such sufficient concentration of the species of interest in the case of NMR, which holds for the monomer concentration. (2) In the case of the active sites and vinyl end group analyses, the concentrations are relatively low, causing the uncertainty to increase. Three separate measurements were performed for each sample, where the concentration varied slightly from measurement to measurement. The standard deviation calculated on the basis of these three measurements is compared to the inherent NMR integration error, and the larger error is chosen. (3) In the case of the GPC measurements, repeat runs result in minimal scatter such that the GPC curves appear overlapping. This, however, should not be taken as an actual estimate of the experimental error, since the error in the GPC measurements may be systematic rather than random due to various reasons described in the literature.[29] Instead, we assumed that the potential error in the GPC outputs caused by the uncertainty in the dn/dc values, interdetector time, and so forth, amounts to at most a 10% up or down shift of each slice molecular weight and hence the shift of the entire MWD. (This actually translates in the −0.05/+0.04 shifts on log scale).[7] For most of the studied systems, error from the GPC measurements were determined to cause the largest uncertainty in the rate constants, and therefore this method was used to generate the uncertainty reported in this paper.

In the rest of this section we provide first the detailed analysis including fits to the data for each catalyst system, and then a summary of all the rate constants in Table 1.

Zr-THF Catalyst 1. The experimental data along with the kinetic modeling fits are presented in Figure 2.

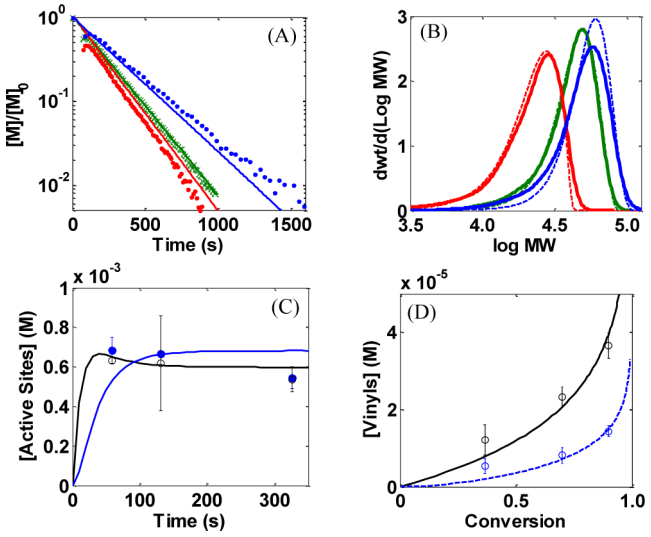

Figure 2. Multiresponse data set with fits for Zr[^{t}Bu-ON^{THF}O]Bn_2/$B(C_6F_5)_3$ catalyst **1**. (A) Monomer consumption of selected NMR scale reactions having catalyst to monomer ratios of 1:100 (red, $[C]_0$ = 3.0 mM, $[M]_0$ = 0.30 M), 1:200 (green, $[C]_0$ = 3.0 mM, $[M]_0$ = 0.60 M), and 1:400 (blue, $[C]_0$ = 1.5 mM, $[M]_0$ = 0.60 M). Symbols are data; solid lines are modeling fits. (B) MWDs of the polymer resulting from the reactions shown in (A). Solid curves are data, dashed curves are fits. (C) Active site counts of selected batch scale reaction with three quenches using MeOD at different reaction times. $[C]_0$ = 3.0 mM, $[M]_0$ = 0.60 M. Black symbols: primary active-site count; blue symbols: secondary active-site count. Solid curves are modeling fits. (D) Vinyl analyses of selected batch scale reaction with three quenches at different reaction time. $[C]_0$ = 3.0 mM, $[M]_0$ = 0.60 M. Black symbols: vinylidene count; blue symbols: vinylene count. Lines represent kinetic modeling fits.

The specific features of this system are (1) very few chain transfer events and (2) catalyst participation is around 50%.

Zr-Pyridine Catalyst 2. The experimental data along with the kinetic modeling fits are presented in Figure 3.

The specific features of this system are (1) catalyst participation around 50%, (2) initiation is fast, i.e., no more than 40 times slower than propagation, and (3) the monomer consumption, i.e., the logarithm of the normalized monomer

dx.doi.org/10.1021/ja401474v | J. Am. Chem. Soc. XXXX, XXX, XXX−XXX

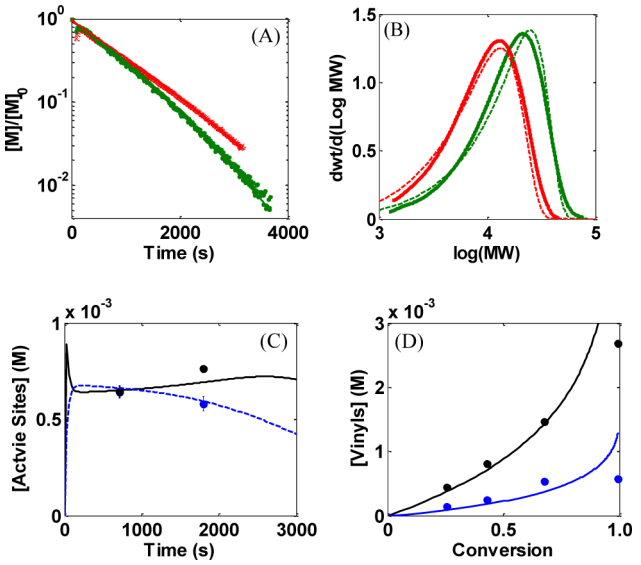

Figure 3. Multiresponse data set with fits for Zr[^{t}Bu-ON^{Py}O]Bn$_2$/B(C_6F_5)$_3$ catalyst **2**. (A) Monomer consumption of selected NMR scale reactions having catalyst to monomer ratios of 1:100 (red, $[C]_0$ = 3.0 mM, $[M]_0$ = 0.30 M), and 1:200 (green, $[C]_0$ = 3.0 mM, $[M]_0$ = 0.60 M). Symbols are data; solid lines are modeling fits. (B) MWDs of the polymer resulting from the reactions shown in (A). Solid curves are data; dashed curves are fits. (C) Active site counts from three selected NMR scale reactions. Each reaction is quenched using MeOD at different reaction time. $[C]_0$ = 3.0 mM; $[M]_0$ = 0.60 M. Black symbols: primary active-site count; blue symbols: secondary active-site count. Solid curves are modeling fits. (D) Vinyl analyses of three selected NMR scale reactions quenched at different reaction time. $[C]_0$ = 3.0 mM; $[M]_0$ = 0.60 M. Black symbols: vinylidene count; blue symbols: vinylene count. Lines represent kinetic modeling fits.

concentration vs time (Figure 3a), appears bent downward. The explanation for this effect is that the overall rate of consumption is controlled by the primary sites, while the secondary sites are dormant. The exit from the secondary sites can happen via two pathways: (1) recovery by normal monomer insertion and (2) monomer independent chain transfer resulting in an activated catalyst ready to initiate a new chain and start consuming monomers. Toward the end of the reaction, when the monomer concentration becomes low, the rate of misinsertion slows down but the second recovery pathway (chain transfer) does not (since it is independent of monomer). As a result, the number of primary sites increases and the number of secondary sites decreases (Figure 3c), producing the apparent acceleration of monomer consumption.

Zr-NMe$_2$ Catalyst 3. The data and model fits for this catalyst have been published in a previous article.[29] The specific features of this system are as follows: (1) Catalyst participation is generally around 45%, although the exact value varied from 20% to 60% depending on the experiment. (2) Initiation is roughly 70 times slower than propagation. (3) Chain transfer occurred moderately frequently, with both vinylidene and vinylene end groups detected. The data suggest that monomer independent pathways, β-H elimination, lead to both types of observed vinyl end groups. (4) The error estimation in the referenced work[29] was calculated via a different method than the one used here. For consistency, the current method has been applied to the data to produce error estimates for the rate constants shown in Table 1. The error estimation is based on the error from the GPC measurement.

Zr-Furan Catalyst 4. The experimental data along with the kinetic modeling fits are presented in Figure 4.

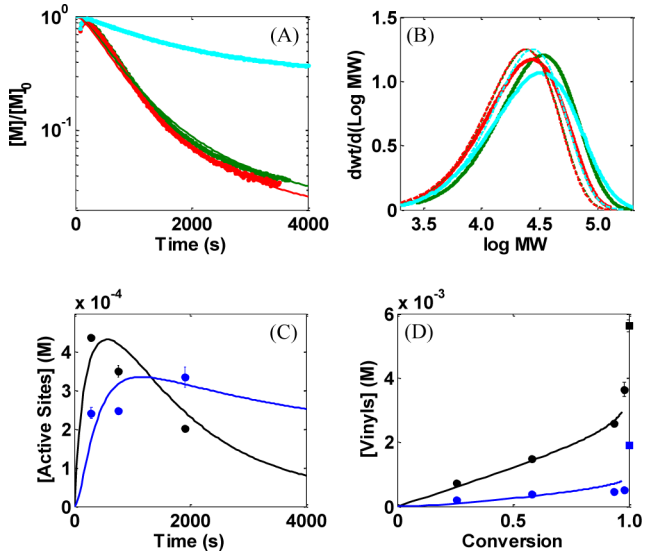

Figure 4. Multiresponse data set with fits for Zr[^{t}Bu-ON^{furan}O]Bn$_2$/B(C_6F_5)$_3$ catalyst **4**. (A) Monomer consumption of selected NMR scale reactions having catalyst to monomer ratios of 1:100 (red, $[C]_0$ = 3.0 mM, $[M]_0$ = 0.30 M), 1:200 (green, $[C]_0$ = 3.0 mM, $[M]_0$ = 0.60 M), and 1:400 (cyan, $[C]_0$ = 1.5 mM, $[M]_0$ = 0.60 M). Symbols are data; solid lines are modeling fits. (B) MWDs of the polymer resulting from the reactions shown in (A). Solid curves are data; dashed curves are fits. (C) Active site counts of selected batch scale reaction with three quenches using MeOD at different reaction time. $[C]_0$ = 3.0 mM; $[M]_0$ = 0.60 M. Black symbols: primary active-site count; blue symbols: secondary active-site count. Solid curves are modeling fits. (D) Vinyl analyses of selected batch scale reaction with three quenches at different reaction time. $[C]_0$ = 3.0 mM; $[M]_0$ = 0.60 M. Black symbols: vinylidene count; blue symbols: vinylene count. Squares are vinyls counts taken after 12 h. Lines represent kinetic modeling fits.

The specific features of this system are as follows: (1) Catalyst participation is around 50%. (2) Initiation is slow, evidenced by the apparent induction period on the monomer consumption curve (Figure 4a). (3) Chain transfer reactions are monomer dependent, β-H transfer to monomer, supported by the following arguments: (a) under different initial catalyst and monomer concentrations, the MWD does not change significantly (Figure 4b); and (b) the relationship between the end group concentrations and monomer conversion during most of the reaction is linear. These two features indicate that the ratio of the chain transfer rate to the propagation rate is a constant independent of the initial concentrations, and that monomer dependent chain transfer reactions control the MW in this system. (4) There is a continuous increase in the end group counts when the batch system is allowed to run overnight after the monomer has already been fully consumed (Figure 4d). It is, hence, concluded that monomer independent chain transfer reaction must take place when there is no monomer, and this chain transfer reaction most likely arises from normal insertion. As mentioned before, this type of chain transfer results in formation of zirconium hydride. However, in order to model the monomer consumption data for this catalyst system, it is necessary for the reinitiation rate constant to be zero, which effectively creates a deactivation pathway that is responsible for the bending observed in the monomer

dx.doi.org/10.1021/ja401474v | J. Am. Chem. Soc. XXXX, XXX, XXX−XXX

consumption curve (Figure 4a) and the drop in primary site count (Figure 4c). It is known that, for some systems, the reinitiation rate is slow for metal hydride.[31] (5) Given that the primary active site count drops and the secondary active sites accumulate, we believe there is no recovery from misinsertion in this system ($k_{reinitiation} \sim 0$).

Zr-SMe Catalyst 5. The experimental data along with the kinetic modeling fits are presented in Figure 5.

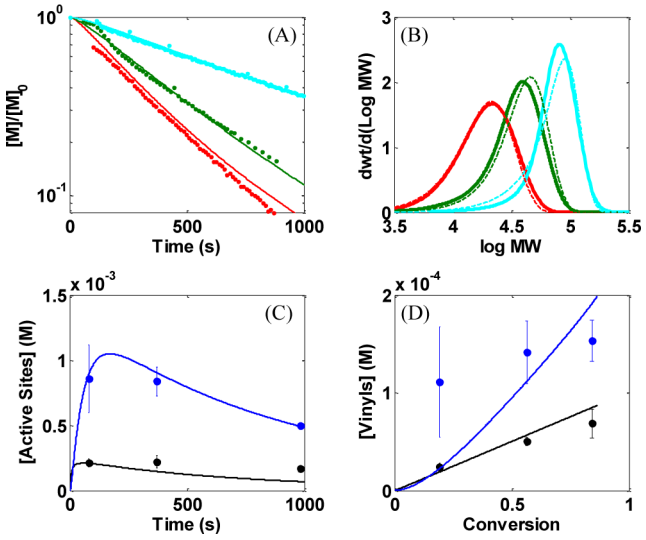

Figure 5. Multiresponse data set with fits for Zr[^{t}Bu-ON^{SMe}O]Bn$_2$/B(C_6F_5)$_3$ catalyst **5**. (A) Monomer consumption of selected NMR scale reactions having catalyst to monomer ratios of 1:100 (red, $[C]_0$ = 3.0 mM, $[M]_0$ = 0.30 M), 1:200 (green, $[C]_0$ = 3.0 mM, $[M]_0$ = 0.60 M), and 1:400 (cyan, $[C]_0$ = 1.5 mM, $[M]_0$ = 0.60 M). Symbols are data; solid lines are modeling fits. (B) MWDs of the polymer resulting from the reactions shown in (A). Solid curves are data, dashed curves are fits. (C) Active site counts of selected batch scale reaction with three quenches using MeOD at different reaction time. $[C]_0$ = 3.0 mM; $[M]_0$ = 0.60 M. Black symbols: primary active site count; blue symbols: secondary active site count. Solid curves are modeling fits. (D) Vinyl analyses of selected batch scale reaction with three quenches at different reaction time. $[C]_0$ = 3.0 mM; $[M]_0$ = 0.60 M. Black symbols: vinylidene count; blue symbols: vinylene count. Squares are vinyls counts taken after 12 h. Lines represent kinetic modeling fits.

The specific features of this system are as follows: (1) Secondary Zr-polymer sites (Zr-CH(Bu)-Polymer) resulting from misinsertion dominate over primary active-sites (Zr-CH_2-Polymer). The model-based explanation is that the k_{mis}/k_p ratio is high while k_{rec}/k_p is low. The values for this catalyst are similar to those for catalyst **1**, where secondary sites are roughly equal to primary sites. (2) Vinylene end groups, which are formed from chain transfer of secondary sites, are more abundant than vinylidene end groups. This is because of the higher concentration of secondary sites rather than a larger $k_{vinylene}$ rate constant. (3) Vinyl groups form via chain transfer to monomer, affording second-order rate constants. The data, however, is not definitive, and a first-order reaction (β-H elimination) cannot be definitively ruled out. In either case, the vinyl concentrations are relatively small, and the effect of the chain transfer rate constants on the responses other than the vinyl end group analysis data (e.g., the MWDs) is small. (4) The total active site concentration (primary plus secondary) decreases over the course of the reaction. In addition, the monomer consumption slows late in the reaction. These behaviors imply a first-order (in catalyst) deactivation reaction. The deactivation rate constant is approximately half of the initiation rate constant, with the result that the total active site concentration remains low throughout the reaction. (5) While 100% of the catalyst is available to initiate (in contrast to the other systems where only a fraction participates), no more than about one-third (ca. 33%) of the zirconium active sites contain a growing polymer chain at any given time.

DISCUSSION

In this study, the complete set of kinetic rate constants for five zirconium amine bis-phenolate catalyst systems have been presented. For each system, a rich data set including MWD has been collected and successfully fitted by comprehensive kinetic modeling. The mechanism of 1-hexene polymerization for these catalysts (**1**−**5**) consists of the following elementary reaction steps: initiation, normal propagation, misinsertion, recovery, and chain transfer. The values of the rate constants are shown in Table 1.

In the first row in Table 1, the Zr−X bond distance as determined by single crystal X-ray crystallography is shown for each catalyst precursor.[10,11,13] Catalysts **1**−**5** are characterized by a progressively longer Zr−X bond distance. From examination of the data given in Table 1, the chain transfer reaction rates (chain transfer following normal insertion, $k_{vinylidene}$, and chain transfer following misinsertion, $k_{vinylene}$) for systems **1**, **2**, and **3** are monomer independent, whereas, for systems **4** and **5**, the predominant chain transfer reactions are monomer dependent. We speculate that once a certain Zr−X bond distance has been reached, there is enough steric freedom to accommodate monomer dependent chain transfer processes as is the case for systems **4** and **5**. As shown in Figure 4d (see caption), when left overnight, system **4** shows an increase in chain transfer products even after all available monomer has been consumed within 1 h suggesting that there is some amount of monomer independent chain transfer (β-H elimination) events taking place. It follows that although monomer dependent chain transfer is the preferred pathway for systems containing a longer Zr-X bond distance, the possibility of monomer independent chain transfer events remains.

While the literature has ample support from empirical observations and semiquantitative measurements that steric constraints of the ligand contribute significantly to chain transfer rates and the mechanism by which chain transfer occurs, i.e., unimolecular β-H elimination versus transfer to monomer,[18] we present a quantitative measure of the rate constants and illustrate at what point a crossover in the chain transfer mechanism occurs. An important point that should not be passed over lightly is that in the analysis of systems **1**−**5** the chain transfer rate constants presented in this work are not obtained just by analysis of vinyl end groups in isolation from all the other rate constants that are pertinent to the catalytic cycle, but rather the full suite of rate constants describing the entire data set for each of the catalyst systems. It is only when this level of quantitative analysis has been employed that one can make definitive QSAR describing how catalyst structure affects properties of the resulting polymer. For example, often in the literature observation of changes in M_w is taken as a direct measure of chain transfer rates as long as activity (TOF) of the catalysts under study remained comparable.[5,18] The assumption in such comparisons is that TOF is a direct measure of k_p and that all other constants did not change. By applying our quantitative analysis methods such assumptions

dx.doi.org/10.1021/ja401474v | J. Am. Chem. Soc. XXXX, XXX, XXX−XXX

and pitfalls that arise from comparing activities rather than rate constants can be eliminated.

A close examination of the unimolecular (β-H elimination) chain transfer rate constants $k_{vinylidene}$ and $k_{vinylene}$ for systems **1**, **2**, and **3** revealed a very intriguing trend. There appears to be a direct correlation between the length of the Zr-X bond distance and $k_{vinylidene}$ and $k_{vinylene}$ (Figure 6). Remarkably, the logarithms

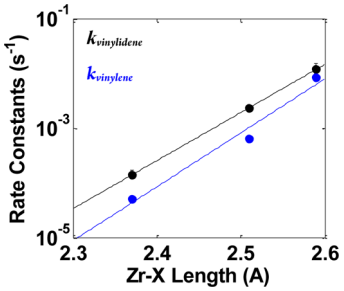

Figure 6. Plot of monomer independent chain transfer rate constants ($k_{vinylidene}$ and $k_{vinylene}$) versus Zr-X bond length for catalysts **1**, **2**, and **3**. Black symbols: chain transfer rate constants from primary sites ($k_{vinylidene}$); blue symbols: chain transfer rate constants from secondary sites ($k_{vinylene}$).

of both chain transfer rate constants appear to depend linearly on the aforementioned bond length. It can be speculated that this increase in bond distance allows for more steric freedom to accommodate the β-hydride agostic interaction necessary for chain transfer to occur, causing an increase in $k_{vinylidene}$ and $k_{vinylene}$ for catalysts **1**, **2**, and **3**. This observation implies that the activation energy, which is proportional to the logarithms of the rate constants at constant temperature, is linearly related to the Zr−X bond length at least for the three systems investigated. Although $k_{vinylidene}$ is always larger than $k_{vinylene}$, as seen in Figure 6, both rate constants are affected in a similar way by the increase of the Zr−X bond length as evidenced by their similar slopes.

Marks and co-workers have probed the effects of using different activators in Zr-based metallocene systems and showed that ion pairing does modulate chain transfer among other rates of polymerization and stereodefects.[26] The work presented in this study has been able to elucidate the role variations have on the rates of chain transfer in a way that can be quantified in terms of the simple Zr−X bond distance. The QSAR presented in Figure 6 is useful because it establishes a relationship for this catalyst family that is based on robust rate constants rather than a relative trend or estimated ordering of rates that represents a composite of elementary reaction steps. Of course, robustly establishing a QSAR model will require the analysis of more systems than just the five reported in this paper; however, these results are the start toward developing a fundamental understanding of the relationship between chemical structure and catalytic activity.

However, in systems **4** and **5** the further increase in the Zr−X bond length does not result in the expected increase in vinyl terminated chains, breaking the aforementioned trend and, moreover, leads to a different chain transfer mechanism: a monomer dependent β-H transfer. To illustrate that this change in the trend is quite significant, we show in Figure 7 the predicted vinyl concentrations for system **4** when it is assumed that the trend would continue. Specifically, the hypothetical values $k_{vinylidene}$ = 0.093 s^{-1} and $k_{vinylene}$ = 0.063 s^{-1} are obtained by extrapolating linearly to the Zr−X bond length for system **4**,

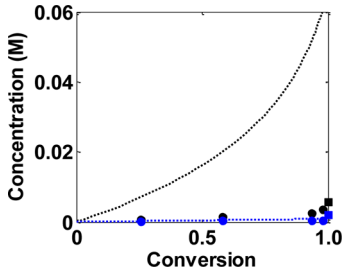

Figure 7. Predicted vinyl formation (dashed curves) using rate constants: k_i = 0.08 M^{-1} s^{-1}, k_p = 8 M^{-1} s^{-1}, $k_{misinsertion}$ = 0.054 M^{-1} s^{-1}, k_{rec} = 0.047 M^{-1} s^{-1}, $k_{vinylidene}$ = 0.093 s^{-1}, and $k_{vinylene}$ = 0.063 s^{-1} for catalyst **4**. Black symbols: measured vinylidene counts; blue symbols: measured vinylene counts. $[C]_0$ = 3.0 mM; $[M]_0$ = 0.60 M.

which is 2.69 Å. The predicted vinylidene concentration is more than 1 order of magnitude higher than the measured experimental value at the end of the reaction. It should be noted that the monomer independent chain transfer is not eliminated completely. As mentioned above, when system **4** was allowed to run for 12 h after the monomer had been consumed an increase in vinyl concentrations was detected.

In the above, we attributed the emergence of the monomer dependent chain transfer mechanism in systems **4** and **5** to increased steric freedom availed by greater Zr−X bond distance. While this may explain the greater ease with which monomer can coordinate to effect chain transfer, it by itself does not explain why the monomer independent reaction should become hindered. We speculate that once the Zr−X distance is large enough (or alternatively the pendent zirconium interaction is weak enough), some other agent, most likely the counterion, may occupy the spot thereby precluding the β-H agostic bond from forming.[26]

Catalyst **5** also exhibits monomer dependent chain transfer with fairly low rate constants. This result is less surprising than that of system **4** as the sulfur atom of the pendant group in **5** is significantly different than the second row pendant ligand atoms (N or O) in **1**−**4** according to HSAB theory. It is speculated that this effect accounts for the mechanistic change observed in system **5**.

The rest of the rate constants shown in Table 1 do not seem to exhibit clear trends with respect to Zr−X bond length. Specifically, k_p is large for systems **1**, **3**, and **5**, and several times lower for catalysts **2** and **4**. This effect alludes to the fact that other catalyst descriptors, i.e., electronic effects, derived from the sp^2 nature of the donor, are perhaps responsible.[10]

Rate constants for misinsertion (k_{mis}) are similar for systems **1**, **2**, and **3**, whereas in the case of **4**, k_{mis} is an order of magnitude slower. For system **5**, k_{mis} is an order of magnitude faster. It stands to reason that the longer Zr−X bond distance would allow for more steric freedom for the misinsertion of monomer resulting in an increased misinsertion rate. However, this line of logic fails to describe catalyst **4**, which appears, yet again, to be an outlier.

Rate of recovery from misinsertion (k_{rec}) is similar for systems **1**, **2**, **3**, and **5**. For system **4**, k_{rec} is zero within the uncertainty of the kinetic analysis. This suggests that the recovery rate for these systems is not governed by sterics.

As discussed in the literature,[10,11] these catalysts produce atactic poly(1-hexene); so, it is not clear if the change in the nature of the pendant effects the degree of tacticity in the resulting polymer product in a way that is easily defined.

dx.doi.org/10.1021/ja401474v | J. Am. Chem. Soc. XXXX, XXX, XXX−XXX

CONCLUSIONS

A comprehensive kinetic study of five catalytic systems based on Zr amine bis-phenolate complexes has been completed, and the relevant rate constants and elementary reaction steps were robustly determined for each system. The mechanism includes initiation, normal propagation, misinsertion, recovery, and chain transfer. The most significant finding was an apparent correlation between the zirconium pendant ligand (Zr–X) bond distance and the rate constants of chain transfer. Specifically, for catalysts **1**–**3**, the logarithm of the chain transfer rate constants ($k_{vinylidene}$ and $k_{vinylene}$) increase linearly with the Zr–X bond distance. Once a certain Zr–X bond distance is reached, the chain transfer mechanism changes from monomer independent β-H elimination to monomer dependent β-H transfer (to monomer), as observed for systems **4** and **5**. This study has also shown that, with the exception of **4**, the rate of misinsertion (k_{mis}) increases for a longer Zr–X bond distance, which is most likely due to an increase in the steric freedom allowing for an increase in misinsertion events, regio errors.

ASSOCIATED CONTENT

Supporting Information

Synthesis of all ligands and precatalysts, as well as a complete set of experimental procedures for each system and kinetic modeling. This material is available free of charge via the Internet at http://pubs.acs.org.

AUTHOR INFORMATION

Corresponding Author

*E-mail: caruther@purdue.edu (J.M.C.); mabuomar@purdue.edu (M.M.A.-O.).

Author Contributions

All authors have given approval to the final version of the manuscript.

Notes

The authors declare no competing financial interest.

ACKNOWLEDGMENTS

Financial support was provided by the U.S. Department of Energy by Grant No. DE-FG02-03ER15466. This research was supported in part by the National Science Foundation through TeraGrid resources provided by Purdue University under grant number TG-CTS070034N. Computing resources were also provided by Information Technology at Purdue.

REFERENCES

(1) Chemical Market Associates, Inc. (CMAI), 2005 *World Polyolefins Analysis*, www.cmaiglobal.com.

(2) (a) Chen, E. Y-X.; Marks, T. J. *Chem. Rev.* **2000**, *100*, 1391–1434. (b) Li, H.; Marks, T. J. *Proc. Natl. Acad. Sci. U.S.A.* **2006**, *103*, 15295–15302.

(3) Manz, T. A.; Phomphrai, K.; Medvedev, G. A.; Krishnamurthy, B. B.; Sharma, S.; Haq, J.; Novstrup, K. A.; Thomson, K. T.; Delgass, W. N.; Caruthers, J. M.; Abu-Omar, M. M. *J. Am. Chem. Soc.* **2007**, *129*, 3776–3777.

(4) (a) Krauledat, H.; Brintzinger, H. H. *Angew. Chem., Int. Ed.* **1990**, *29*, 1412–1413. (b) Piers, W. E.; Bercaw, J. E. *J. Am. Chem. Soc.* **1990**, *112*, 9406–9707. (c) Coates, G. W.; Waymouth, R. M. *J. Am. Chem. Soc.* **1991**, *113*, 6270–6271.

(5) Britovsek, G. J. P.; Gibson, V. C.; Wass, D. F. *Angew. Chem., Int. Ed.* **1999**, *38*, 428–447.

(6) Arriola, D. J.; Carnahan, E. M.; Hustad, P. D.; Kuhlman, R. L.; Wenzel, T. T. *Science* **2006**, *312*, 714–719.

(7) Novstrup, K. A.; Travia, N. E.; Medvedev, G. A.; Stanciu, C.; Switzer, J. M.; Thomson, K. T.; Delgass, W. N.; Abu-Omar, M. M.; Caruthers, J. M. *J. Am. Chem. Soc.* **2010**, *132*, 558–566.

(8) Liu, Z. X.; Somsook, E.; White, C. B.; Rosaaen, K. A.; Landis, C. R. *J. Am. Chem. Soc.* **2001**, *123*, 11193–11207.

(9) (a) Angermund, K.; Fink, G.; Jensen, V. R.; Kleinschmidt, R. *Chem. Rev.* **2000**, *100*, 1457–1470. (b) Bochmann, M. *J. Organomet. Chem.* **2004**, *689*, 3982–3998. (c) Mohring, P. C.; Coville, N. J. *Coord. Chem. Rev.* **2006**, *250*, 18–35. (d) Wang, B. *Coord. Chem. Rev.* **2006**, *250*, 242–258.

(10) Tshuva, E. Y.; Goldberg, I.; Kol, M.; Goldschmidt, Z. *Organometallics* **2001**, *20*, 3017–3028.

(11) Tshuva, E. Y.; Groysman, S.; Goldberg, I.; Kol, M.; Goldschmidt, Z. *Organometallics* **2002**, *21*, 662–670.

(12) Kerton, F. M.; Holloway, S.; Power, A.; Soper, R. G.; Sheridan, K.; Lynam, J. M.; Whitwood, A. C.; Willans, C. E. *Can. J. Chem.* **2008**, *86*, 435–443.

(13) Groysman, S.; Goldberg, I.; Kol, M.; Genizi, E.; Goldschmidt, Z. *Organometallics* **2003**, *22*, 3013–3015.

(14) (a) Gahleitner, M.; Severn, J. R. *Designing Polymer Properties*. In *Tailor-Made Polymers*; Wiley-VCH Verlag GmbH & Co., 2008. (b) Resconi, L.; Cavallo, L.; Fait, A.; Piemontesi, F. *Chem. Rev.* **2000**, *100*, 1253–1346.

(15) Resconi, L.; Piemontesi, F.; Franciscono, G.; Abis, L.; Fiorani, T. *J. Am. Chem. Soc.* **1992**, *114*, 1025–1032.

(16) Mogstad, A.-L.; Waymouth, R. M. *Macromolecules* **1992**, *25*, 2282–2284.

(17) Coates, G. W.; Hustad, P. D.; Reinartz, S. *Angew. Chem., Int. Ed.* **2002**, *41*, 2236–2257.

(18) Mecking, S. *Angew. Chem., Int. Ed.* **2001**, *40*, 534–540 and references therein.

(19) Agapie, T.; Henling, L. M.; DiPasquale, A. G.; Rheingold, A. L.; Bercaw, J. E. *Organometallics* **2008**, *27*, 6245–6256.

(20) Margl, P.; Deng, L. Q.; Ziegler, T. *J. Am. Chem. Soc.* **1999**, *121*, 154–162.

(21) Busico, V.; Cipullo, R.; Friederichs, N.; Ronca, S.; Talarico, G.; Togrou, M.; Wang, B. *Macromolecules* **2004**, *37*, 8201–8203.

(22) Camacho, D. H.; Guan, Z. B. *Macromolecules* **2005**, *38*, 2544–2546.

(23) (a) Meinhard, D.; Wegner, M.; Kipiani, G.; Hearley, A.; Reuter, P.; Fischer, S.; Marti, O.; Rieger, B. *J. Am. Chem. Soc.* **2007**, *129*, 9182–9191. (b) Anselment, T. M. J.; Wichmann, C.; Anderson, C. E.; Herdtweck, E.; Rieger, B. *Organometallics* **2011**, *30*, 6602–6611.

(24) Doi, Y.; Ueki, S.; Keii, T. *Macromolecules* **1979**, *12*, 814–819.

(25) Naga, N.; Mizunuma, K. *Polymer* **1998**, *39*, 5059–5067.

(26) Chen, M.-C.; Roberts, J. A. S.; Marks, T. J. *J. Am. Chem. Soc.* **2004**, *126*, 4605–4625.

(27) Groysman, S.; Goldberg, I.; Kol, M.; Genizi, E.; Goldschmidt, Z. *Inorg. Chim. Acta* **2003**, *345*, 137–144.

(28) Tshuva, E. Y.; Gendeziuk, N.; Kol, M. *Tetrahedron Lett.* **2001**, *42*, 6405–6407.

(29) Switzer, J. M.; Travia, N. E.; Steelman, D. K.; Medvedev, G. A.; Thomson, K. T.; Delgass, W. N.; Abu-Omar, M. M.; Caruthers, J. M. *Macromolecules* **2012**, *45*, 4978–4988.

(30) Liu, Z.; Somsook, E.; Landis, C. R. *J. Am. Chem. Soc.* **2001**, *123*, 2915–2916.

(31) Christianson, M. D.; Tan, E. H. P.; Landis, C. R. *J. Am. Chem. Soc.* **2010**, *132*, 11461–11463.